Since January 2020 Elsevier has created a COVID-19 resource centre with free information in English and Mandarin on the novel coronavirus COVID-19. The COVID-19 resource centre is hosted on Elsevier Connect, the company's public news and information website.

Medical Hypotheses 155 (2021) 110656

Contents lists available at ScienceDirect

Medical Hypotheses

journal homepage: www.elsevier.com/locate/mehy

Drug-repurposing against COVID-19 by targeting a key signaling pathway: An *in silico* study

Ki Kwang Oh, Md. Adnan, Dong Ha Cho *

Department of Bio-Health Convergence, College of Biomedical Science, Kangwon National University, Chuncheon 24341, South Korea

ARTICLE INFO

Keywords:
COVID-19
Estrogen signaling pathway
AKT1-HSP90AB1-BCL2
Akti-1/2-HSP990-S55746
Anti-inflammatory effects

ABSTRACT

Currently, a plethora of information has been accumulated concerning COVID-19, including the transmission pathway of SARs-CoV-2. Thus, we retrieved targets associated with the development of COVID-19 via PubChem. A total of 517 targets were identified, and signaling pathways responded after infection of SARs-CoV-2 in humans constructed a bubble chart using RPackage. The bubble chart result suggested that the key signaling pathway against COVID-19 was the estrogen signaling pathway associated with AKT1, HSP90AB1, BCL2 targets. The three targets have the strongest affinity with three ligands-Akti-1/2, HSP990, S55746, respectively. In conclusion, this work provides three key elements to alleviate COVID-19 symptoms might be anti-inflammatory effects on SARs-CoV-2-infected lung cells.

Introduction

COVID-19, an invasion of SARs-CoV-2, was generated by unknown etiology was first announced at Wuhan in Hubei Province, China, and notified to World Health Organization (WHO) by the Wuhan Municipal Health Commission on 31 December 2019 [1]. At present, there is no treatment to unravel coronavirus disease symptoms such as cough, fever, fatigue, and shortness of breath [2,3]. A report suggests that drug repurposing is the most efficient way to develop new indications in aspects of the economic approach [4]. The first strategy to develop COVID-19 drugs is to investigate a new therapeutic efficacy from existing drugs, which can rapidly scan their effectiveness by defining unexpected side effects [5]. To understand infection and development of COVID-19, deciphering signaling pathways that responded by SARS-CoV-2 invasion at the pharmacological level is of pivotal significance [6]. Understanding existing drugs' targets and physicochemical properties is highly useful for promoting the drug repurposing against COVID-19 [7]. An *in silico* study for drug repurposing provided new drug-target relationships; likewise, this approach is also applicable against COVID-19 [8]. Therefore, this study has focused on establishing targets, ligands associated with a key signaling pathway against COVID-19 via an *in silico* study.

Hypothesis

The targets associated with COVID-19 were identified via PubChem, which is considered to be therapeutically relevant. We hypothesize that the targets can provide key signaling pathway(s) and key target protein (s) along with Rich Factor indicated the percentage of the number of Differentially Expressed Genes (DEGs) to alleviate COVID-19, thereby, can obtain the most promising therapeutic ligands via molecular docking test.

Method

The targets related to COVID-19 were obtained through PubChem (https://pubchem.ncbi.nlm.nih.gov/), which are elements to identify signaling pathways against COVID-19. The targets were analyzed by STRING (https://string-db.org/) database [9], RPackage software was used to plot a bubble chart. Through the bubble chart based on Rich Factor, a key signaling pathway against COVID-19 demonstrated. In addition, targets connected directly to the key signaling pathway were identified on the STRING (https://string-db.org/) database. We prepared for existing positive ligands bound to targets connected to the key signaling pathway. The confirmed ligands were converted .sdf from PubChem into .pdb format using Pymol, and the ligand molecules were converted into .pdbqt format through Autodock. Also, PDB ID of targets were identified via RCSB PDB (https://www.rcsb.org/), which was

* Corresponding author.
E-mail address: chodh@kangwon.ac.kr (D.H. Cho).

https://doi.org/10.1016/j.mehy.2021.110656
Received 28 May 2021; Received in revised form 12 July 2021; Accepted 31 July 2021
Available online 9 August 2021

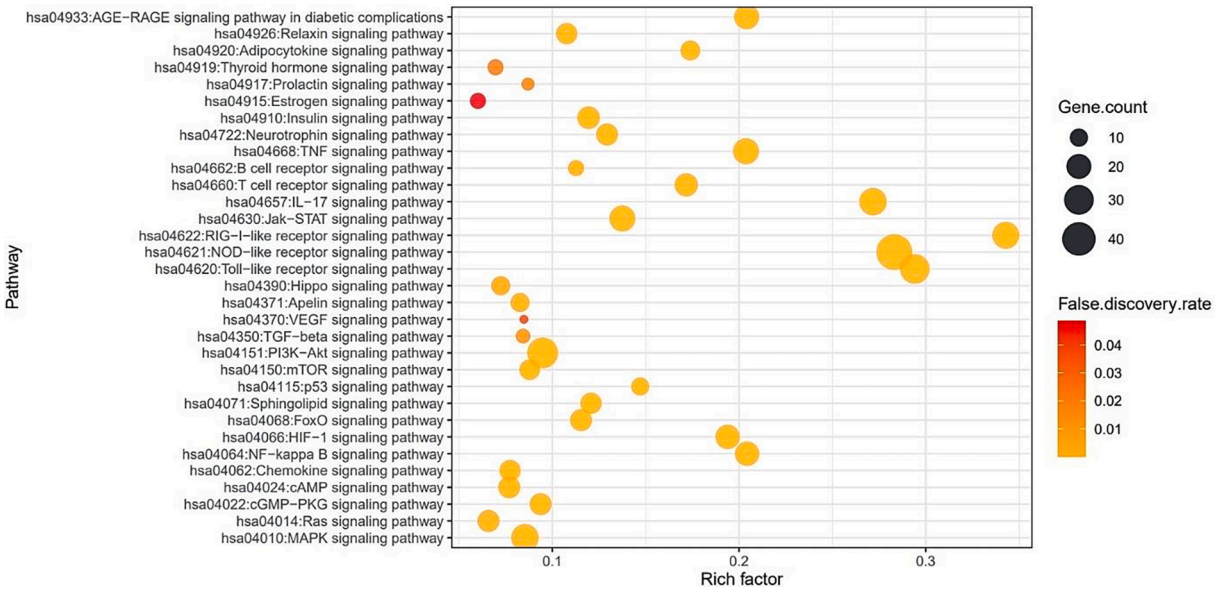

Fig. 1. Bubble chart of 32 signaling pathways associated with COVID-19.

Table 1
Physicochemical properties of chemical compounds for good oral bioavailability and cell membrane permeability.

No.	Compounds	Lipinski Rules				Lipinski's Violations	Bioavailability Score	TPSA(Å^2)
		MW <500	HBA <10	HBD ≤5	MLog P ≤4.15	≤1	>0.1	<140
1	Luteolin	286.24	6	4	−0.03	0	0.55	111.13
2	Akti-1/2	551.64	5	2	3.6	1	0.55	95.49
3	MK-2206 2HCl	480.39	4	2	4.05	0	0.55	89.07
4	Uprosertib (GSK2141795)	429.25	6	2	2.64	0	0.55	86.08
5	Miransertib (ARQ-092)	432.52	4	2	3.14	0	0.55	95.64
6	Afuresertib (GSK2110183)	427.32	4	2	3.08	0	0.55	101.18
7	HSP990 (NVP-HSP990)	379.39	6	2	1.8	0	0.55	103.02
8	SNX-2112 (PF-04928473)	464.48	7	3	2.44	0	0.55	110.24
9	URMC-099	421.54	3	2	3.08	0	0.55	50.95
10	Masitinib (AB1010)	498.64	5	2	2.37	0	0.55	101.63
11	PF-04929113 (SNX-5422)	524.53	9	3	2.02	1	0.55	142.33
12	XL888	503.64	4	3	2.44	1	0.55	117.42
13	NMS-E973	454.43	9	3	0.41	1	0.55	153.88
14	Grp94 Inhibitor-1	352.47	2	3	3.04	0	0.55	75.35
15	Ganetespib (STA-9090)	364.40	4	3	2.66	0	0.55	96.07
16	VER-50589	388.80	6	3	1.58	0	0.55	104.82
17	Onalespib (AT13387)	409.52	5	2	2.09	0	0.55	67.25
18	TAS-116	454.53	5	1	2.13	0	0.55	109.44
19	Luminespib (NVP-AUY922)	465.54	7	3	1.54	0	0.55	108.06
20	NMS-873	520.67	6	0	3.73	1	0.55	120.65
21	CH5138303	415.90	5	2	1.31	0	0.55	142.31
22	VER-49009	387.82	5	4	1.58	0	0.55	107.47
23	BIIB021	318.76	5	1	0.5	0	0.55	91.74
24	PU-H71	512.37	6	2	2.12	1	0.55	125.41
25	NVP-BEP800	480.41	5	2	2.81	0	0.55	121.61
26	Ethoxyquin	217.31	1	1	2.73	0	0.55	21.26
27	Cinobufagin	442.54	6	1	3.08	0	0.55	89.27
28	Nodakenetin	246.26	4	1	1.6	0	0.55	59.67
29	S55746	710.82	7	1	3.67	1	0.55	96.71
30	A-1331852	658.81	6	2	3.91	1	0.56	141.48
31	WEHI-539 HCl	620.18	7	3	3.9	1	0.55	179.2
32	BTSA1	430.51	5	1	3.55	0	0.55	144.77
33	Unesbulin (PTC596)	420.34	8	2	4.08	0	0.55	81.65
34	Berberine chloride hydrate	389.83	5	1	1.6	0	0.55	50.03
35	Berberine chloride (NSC 646666)	371.81	4	0	2.41	0	0.55	40.8
36	Obatoclax Mesylate (GX15-070)	413.49	5	3	0.82	0	0.55	115.92
37	Mifepristone (RU486)	429.59	2	1	4.65	1	0.55	40.54
38	BAM7	405.47	5	1	2.77	0	0.55	112.87
39	BDA-366	423.50	5	3	0.54	0	0.55	94.2
40	BAI1	540.12	3	2	3.56	1	0.55	40.43
41	HA14-1	409.23	6	1	1.44	0	0.55	111.64

MW, Molecular Weight (g/mol); HBA, Hydrogen Bond Acceptor; HBD, Hydrogen Bond Donor; LogP, Lipophilicity; Bioavailability Score, The ability of a drug or other substance to be absorbed and used by the body; TPSA, Topological Polar Surface Area.

Table 2
Binding energy of existing positive ligands on AKT1 (PDB ID: 3O96).

Protein	Ligand	PubChem ID	Binding energy (kcal/mol)	Grid box		Hydrogen Bond Interactions		Hydrophobic Interactions
				Center	Dimension	Amino Acid Residue	Distance (Å)	Amino Acid Residue
AKT1 (PDB ID: 3O96)	*Luteolin [22]	5,280,445	−8.7	X = 6.313 Y = -7.926 Z = 17.198	Size X = 40 Size Y = 40 Size Z = 40	Asn199, Trp80, Ser56, Asn53	3.23, 3.27, 3.04 3.01, 2.88	Phe225, Gln59, Leu78, Ala58, Gln79, Val201
	Akti-1/2	135,398,501	−9.2	X = 6.313 Y = -7.926 Z = 17.198	Size X = 40 Size Y = 40 Size Z = 40	Glu49	2.88	Lys39, Pro42, Tyr38, Ser396, Arg328, Tyr326, Phe55, Ile36, Gln43, Glu40
	MK-2206 2HCl	46,930,998	−8.8	X = 6.313 Y = -7.926 Z = 17.198	Size X = 40 Size Y = 40 Size Z = 40	Tyr263, Asn204, Gln414	2.84, 3.17, 3.22	Trp413, Tyr417, Glu267, Asp262, Ser259, His207, Met403
	Uprosertib (GSK2141795)	51,042,438	−7.7	X = 6.313 Y = -7.926 Z = 17.198	Size X = 40 Size Y = 40 Size Z = 40	Tyr326, Gly37, Ala329	3.15, 2.90, 3.24	Gly394, Arg328, Pro51, Leu52, Ile36, Tyr38, Phe55, Asp325, Gly327, Lys389, Pro388
	Miransertib (ARQ-092)	53,262,401	−7.7	X = 6.313 Y = -7.926 Z = 17.198	Size X = 40 Size Y = 40 Size Z = 40	Phe293	3.23	Tyr229, Met281, Leu156, Glu234, Phe236, Glu278, Leu295, Glu298
	Afuresertib (GSK2110183)	46,843,057	−7.6	X = 6.313 Y = -7.926 Z = 17.198	Size X = 40 Size Y = 40 Size Z = 40	Ala329, Arg328, Gly37	3.15, 3.20, 3.00	Gly394, Gly327, Tyr38, Pro51, Ala50, Ile36, Asp325, Phe55, Tyr326, Pro388, Lys389

*Luteolin: A natural inhibitor on AKT1.

selected as .pdb format were converted .pdbqt format via Autodock (http://autodock.scripps.edu/). The existing positive ligands were docked with targets utilizing autodock4 by setting up 4 energy ranges and 8 exhaustiveness as default to obtain 10 different poses of ligand molecules [10]. The ligand molecules were docked with targets using autodock4 by setting 8 exhaustiveness as default to obtain 10 different poses of ligand molecules. The center (a position of the middle coordinate point) in the target was X: −7.586, Y: 7.516, Z: 21.954 on BCL2 (PDB ID: 5VAU), X: 6.313, Y: −7.926, Z: 17.198 on AKT1 (PDB ID: 3O96), and X: 160.556, Y: 164.529, Z: 173.251 on HSP90AB1 (PDB ID: 5FWL). The grid box size was set to 40 Å × 40 Å × 40 Å. The 2D binding interactions were used with LigPlot+ v.2.2 (https://www.ebi.ac.uk/thornton-srv/software/LigPlus/). After docking, ligands of the lowest binding energy (highest affinity) were selected to visualize the ligand-target interaction in Pymol.

Result

A total of 517 human genes responded to SARs-CoV infection obtained via PubChem (https://pubchem.ncbi.nlm.nih.gov/). On RPackage software, a scatter plot based on the Rich Factor of signaling pathways in STRING (https://string-db.org/) database indicated that the estrogen signaling pathway was the lowest Rich factor (0.060) among 32 signaling pathways associated with SARS-CoV-2 infection (Fig. 1). The "Rich factor" defines that the ratio of the DEGs number and the number of genes have been annotated in the signaling pathways which have significant features with<0.05 (False discovery rate). Thus, the dampening of the estrogen signaling pathway might be a hub signaling pathway against COVID-19. The target information of 32 signaling pathways is listed in Supplementary Table S1. The targets related to the estrogen signaling pathway were BCL2, AKT1, HSP90AB1, OPRM1, ATF2, ATF4, CTSD, and NOS3. Among the number of 8 targets, only three targets (BCL2, AKT1, HSP90AB1) were identified as existing inhibitors. The existing inhibitors were identified by retrieving literature, which was confirmed by Lipinski's rule (molecular weight ≤500 g/mol; Moriguchi octanol–water partition coefficient ≤4.15; the number of nitrogen or oxygen ≤10; the number of NH or OH ≤5) via the SwissADME database [11]. Additionally, cell membrane permeability is generally limited when the topological polar surface area (TPSA) value exceeds 140 $Å^2$ [12] (Table 1).

Our molecular docking test demonstrated that Akti-1/2 (PubChem ID: 135398501) among 6 existing positive ligands (including a natural ligand: Luteolin) is the highest affinity of −9.2 kcal/mol on AKT1 (PDB ID: 3O96) (Table 2). NVP-HSP990 (PubChem ID: 46216556) among ~~24~~ 20 existing positive ligands is the most excellent binding energy of −10.9 kcal/mol on HSP90AB1 (PDB ID:5FWL) (Table 3). S55746 (PubChem ID: 71654876) among 16 existing positive ligands (Including natural inhibitors: Cinobufagin; Nodakenetin) is the greatest affinity of −14.0 kcal/mol on BCL2 (PDB ID: 5VAU) (Table3). Structures of the most promising ligands on each target are shown in Fig. 2 and displayed in Fig. 3(A), (B), (C).

Table 3
Binding energy of existing positive ligands on HSP90AB1 (PDB ID: 5FWL).

Protein	Ligand	PubChem ID	Binding energy (kcal/mol)	Grid box		Hydrogen Bond Interactions		Hydrophobic Interactions
				Center	Dimension	Amino Acid Residue	Distance (Å)	Amino Acid Residue
HSP90AB1(PDB ID:5FWL)	HSP990 (NVP-HSP990)	46,216,556	−10.9	X = 166.556 Y = 164.529 Z = 173.251	Size X = 40 Size Y = 40 Size Z = 40	Lys406, Ser445	3.24, 3.02	Asn447, Asp14, Phe29, Glu443, Asp444, Glu372, Tyr373, Ile370, Pro371, Arg405, Val409, Thr446
	SNX-2112 (PF-04928473)	24,772,860	−10.6	X = 166.556 Y = 164.529 Z = 173.251	Size X = 40 Size Y = 40 Size Z = 40	Asn447, Lys350	2.98, 2.92	Thr446, Phe29, Asp444, Glu443, Gly44, Gly45, Asp367, Glu372, Pro371, Ile370, Arg405, Asp14
	URMC-099	54,764,565	−10.5	X = 166.556 Y = 164.529 Z = 173.251	Size X = 40 Size Y = 40 Size Z = 40	Thr149	3.26	Glu431, Lys435, Ala432, Leu343, Pro340, Ala339, Asp613, Phe341, Asp342, Thr153, Lys155, Val96, Glu94, Glu345, Leu611, Phe344, Ser434
	Masitinib (AB1010)	10,074,640	−10.4	X = 166.556 Y = 164.529 Z = 173.251	Size X = 40 Size Y = 40 Size Z = 40	N/A	N/A	Lys348, Leu343, Asn375, Thr90, Glu372, Tyr373, Asp14, Arg405, Pro371, Asp444, Glu443, Lys347, Gly44, Phe93, Asn346, Leu91, Glu345
	PF-04929113 (SNX-5422)	44,195,571	−10.0	X = 166.556 Y = 164.529 Z = 173.251	Size X = 40 Size Y = 40 Size Z = 40	Arg405, Lys350, Thr25	3.28, 3.04, 3.03	Ile370, Pro371, Asp367, Glu372, Gly45, Gly44, Glu443, Ala26, Asp444, Phe29, Thr446, Asp14
	XL888	57,748,689	−10.0	X = 166.556 Y = 164.529 Z = 173.251	Size X = 40 Size Y = 40 Size Z = 40	N/A	N/A	Asn346, Glu345, Phe344, Leu439, Asn436, Leu343, Glu372, Glu443, Asp444, Leu91, Phe93, Lys347, Gly43, Asn346, Gly44, Gly42, Thr90
	NMS-E973	135,566,652	−9.8	X = 166.556 Y = 164.529 Z = 173.251	Size X = 40 Size Y = 40 Size Z = 40	Glu443, Thr25, Glu372, Lys350	3.30, 3.12,2.98, 2.98	Ser445, Phe29, Ala26, Asp444, Asp14, Thr446, Pro371, Val409. His95
	Grp94 Inhibitor-1	137,321,151	−9.6	X = 166.556 Y = 164.529 Z = 173.251	Size X = 40 Size Y = 40 Size Z = 40	Leu611	3.00	Glu94, Arg612, Phe93, Phe344, Lys435, Ala432, Glu431, Ala339, Leu343, Pro340, Phe341, Asp613,

(*continued on next page*)

Table 3 (*continued*)

Protein	Ligand	PubChem ID	Binding energy (kcal/mol)	Grid box		Hydrogen Bond Interactions		Hydrophobic Interactions
				Center	Dimension	Amino Acid Residue	Distance (Å)	Amino Acid Residue
								Val96, Met620, Thr616
	Ganetespib (STA-9090)	135,564,985	−9.5	X = 166.556 Y = 164.529 Z = 173.251	Size X = 40 Size Y = 40 Size Z = 40	Arg612	2,90	Val96, Thr616, Ser150, Met620, Gly151, Thr149, Thr153, Phe341, Lys155, Leu611, Asp613, Phe344, Glu345, Phe93
	VER-50589	135,446,210	−9.4	X = 166.556 Y = 164.529 Z = 173.251	Size X = 40 Size Y = 40 Size Z = 40	Glu372, Thr25, Ser445 Asp14	2.96, 3.02, (2.70, 3.02) 3.16	Glu16, Phe29, Thr446, Val409, Asn447, Lys406, Asp444, Tyr373, Pro371, Glu443
	Onalespib (AT13387)	11,955,716	−9.4	X = 166.556 Y = 164.529 Z = 173.251	Size X = 40 Size Y = 40 Size Z = 40	Gly42	3.15	Thr90, Glu372, Phe344, Asn346, Glu345, Leu439, Leu343, Val92, Phe93, Lys347, Glu443, Leu91, Gly43, Gly44
	TAS-116	67,501,411	−9.3	X = 166.556 Y = 164.529 Z = 173.251	Size X = 40 Size Y = 40 Size Z = 40	Tyr373, Asp444, Thr19	2.91, 2.84, 3.02	Val409, Pro371, Asp14, Asn447, Gly44, Glu16, Thr25, Phe29, Lys348, Arg405, Glu443, Glu372
	Luminespib (NVP-AUY922)	135,539,077	−9.2	X = 166.556 Y = 164.529 Z = 173.251	Size X = 40 Size Y = 40 Size Z = 40	Thr25, Glu443	2.96, 3.29	His95, Ala26, Ser445, Thr446, Phe29, Asp14, Asp444, Arg405, Tyr373, Pro371, Glu16
	NMS-873	71,521,142	−9.2	X = 166.556 Y = 164.529 Z = 173.251	Size X = 40 Size Y = 40 Size Z = 40	N/A	N/A	Phe29, Glu16, Lys347, Gly44, Gly43, Phe93, Asn346, Leu343, Thr90, Glu372, Pro371, Glu443
	CH5138303	25,066,238	−9.1	X = 166.556 Y = 164.529 Z = 173.251	Size X = 40 Size Y = 40 Size Z = 40	Phe93, His442, Leu343, Asn375, Gly43	2.80, 3.14, 3.05 2.81, 2.80	Val92, Leu91, Asn346, Thr90, Gly42, Lys348, Glu345, Gly44, Gly46, Glu372, Lys347, Glu443
	VER-49009	4,369,536	−9.1	X = 166.556 Y = 164.529 Z = 173.251	Size X = 40 Size Y = 40 Size Z = 40	Glu372, Thr25, Ser445, Asp14	2.97, 3.13, 2.86, 3.08	Glu443, Thr446, Val409, Asn447, Lys406, Asp444, Tyr373, Pro371, Phe29, Glu16
	BIIB021	16,736,529	−8.0	X = 166.556 Y = 164.529 Z = 173.251	Size X = 40 Size Y = 40 Size Z = 40	Glu372	3.22	Asp444, Thr446, Phe29, Tyr373, Glu443, Gly44, Asp367, Arg405, Pro371, Asp14
	PU-H71	9,549,213	−8.0		Size X = 40	Asn447, Arg405	2.99, 3.09	

(*continued on next page*)

Table 3 (*continued*)

Protein	Ligand	PubChem ID	Binding energy (kcal/mol)	Grid box		Hydrogen Bond Interactions		Hydrophobic Interactions
				Center	Dimension	Amino Acid Residue	Distance (Å)	Amino Acid Residue
				X = 166.556 Y = 164.529 Z = 173.251	Size Y = 40 Size Z = 40			Thr446, Asp444, Glu443, Tyr373, Gly44, Glu16, Pro371, Val409, Asp14
	NVP-BEP800	25,210,273	−7.8	X = 166.556 Y = 164.529 Z = 173.251	Size X = 40 Size Y = 40 Size Z = 40	Asp367, Gly45	2.86, 2.89	Glu443, Phe29, Gly44, Glu16, Lys347, Lys348, Asp444, Glu372, Tyr373, Pro371, Asp14, Arg405
	Ethoxyquin	3293	−7.4	X = 166.556 Y = 164.529 Z = 173.251	Size X = 40 Size Y = 40 Size Z = 40	N/A	N/A	Phe344, Asn436, Asn346, Glu443, Val89, Pro40, Arg85, Tyr373, Leu439, Leu611, Glu372, Leu343

Discussion

The targets associated with COVID-19 suggested that therapeutic effects against SARs-CoV-2 was directly connected with 32 signaling pathways, estrogen signaling pathway was identified as the uppermost signaling pathway. The number of 3 targets (AKT1, HSP90AB1, BCL2) related directly to the estrogen signaling pathway was measured the therapeutic value via molecular docking test (MDT) (Table 4).

A report demonstrated that estrogen induces significantly the production of proinflammatory cytokines such as Interleukin-6 (IL-6), tumor necrosis factor-alpha (TNF-α), Interleukin-1β (IL-1β), NF-kB in lung cells [13]. Most recently, female cancer patients under SERM (Selective estrogen receptor modulator) have a higher risk of SARs-CoV-2 infection. Furthermore, the loss of estrogens in these patients blocked the symptoms of COVID-19 [14]. This report is in line with our study hypothesis.

AKT1 is a vital target to diminish the lung injury, damage, hyperactivation of AKT1 recruited memory CD8+ T-cell [15]. Also, AKT isoforms 1 and 2 play an essential function in immune cell stimulation and migration, which is deeply involved in the systemic and local inflammation against COVID-19 [16]. It implies that the inactivation of AKT1 on COVID-19 may attune its severity. Among the selective AKT1 inhibitors, we suggest that Akti-1/2 (PubChem ID: 135398501) might be a powerful, potent ligand to fight against COVID-19.

Heat Shock Protein 90 (HSP90) blocker dampens replication of SARs-CoV-2 and cytokine mRNA levels in human airway epithelial tissues [17]. The inhibition of HSP90 suppresses pro-inflammatory cytokines elements such as TNF and IL-1β [18]. Additionally, a report indicated that HSP90 inhibitors might alleviate acute respiratory distress syndrome (ARDS) and other vascular inflammatory diseases [19]. We suggest that HSP990 (PubChem ID: 46216556) is a potential ligand to lessen COVID-19 symptoms.

BCL2 proteins are associated with SARs-CoV-2-induced apoptosis can be inverse partly through the expression of BCL2, suggesting that BCL2 is a mediator to control either apoptosis or survival of SARs-CoV-2-infected lung cells [20]. The SARs-CoV-2-infected cells recruit cytokines to induce the activation of $CD4^+$ T cells, $CD14^+$ and $CD16^+$ monocytes, leading to excessive inflammatory responses [21]. It implies that apoptosis of SARs-CoV-2-infected cells is an optimal strategy to alleviate COVID-19 symptoms. We suggest that S55746 (PubChem ID: 46216556) is a promising ligand on BCL2 against COVID-19. The location of each target is indicated on the KEGG pathway (Fig. 4). Therefore, the key pharmacological mechanism of COVID-19 is to block inflammation by inactivating the estrogen signaling pathway in the lungs (Fig. 5).

Conclusion

In conclusion, the inactivation of the estrogen signaling pathway in

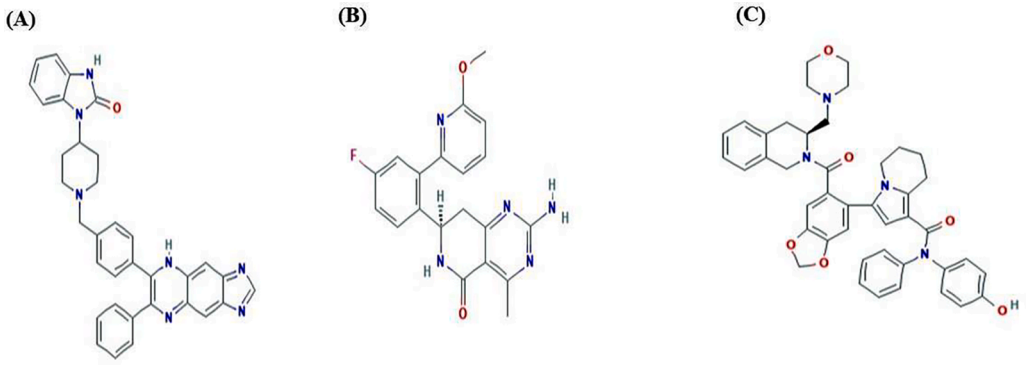

Fig. 2. The 2D structure of three promising ligands against COVID-19. (A) Akti-1/2 (PubChem ID: 135398501). (B) HSP990 (PubChem ID: 46216556). (C) S55746 (PubChem ID: 71654876).

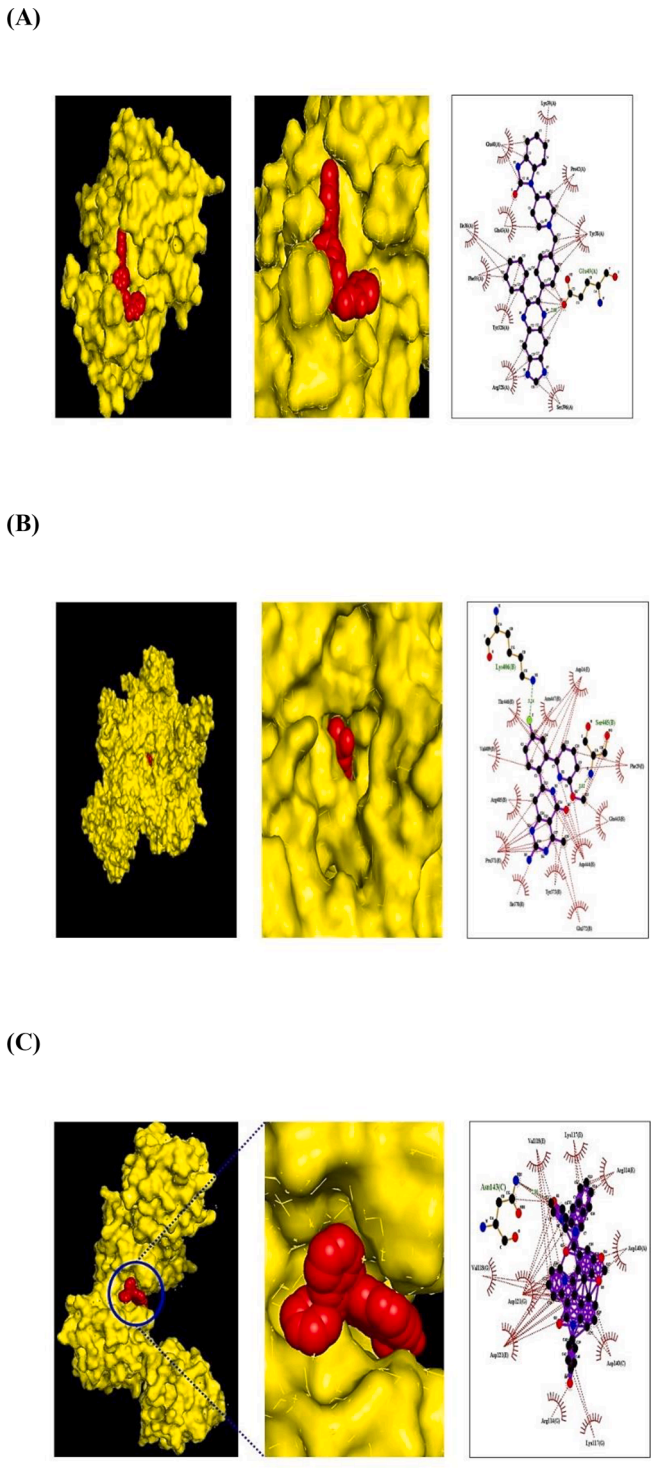

Fig. 3. Molecular docking interaction between ligands and targets. (A) Akti-1/2 on AKT1 (PDB ID: PDB ID: 3O96). (B) HSP990 (PubChem ID: 46216556) on HSP90AB1 (PDB ID:5FWL). (C) S55746 (PubChem ID: 71654876) on BCL2 (PDB ID: 5VAU).

lung cells might dampen the COVID-19 severity. The three targets (AKT1, HSP90AB1, BCL2) are related directly to the estrogen signaling pathway with the development of COVID-19 symptoms. We suggest that the most 3 potent ligands (Akti-1/2, HSP990, and S55746) might be promising alleviators for COVID-19 patients. This work provides that mechanism studies via MDT shed light on signaling pathways related directly to COVID-19 and a research basis for elucidating three elements: targets-ligands-signaling pathways.

Funding

This research did not receive any specific grant from funding agencies in the public, commercial, or not-for-profit sectors.

Declaration of Competing Interest

The authors declare that they have no known competing financial interests or personal relationships that could have appeared to influence

Table 4
Binding energy of existing positive ligands on BCL2 (PDB ID: 5VAU).

Protein	Ligand	PubChem ID	Binding energy (kcal/mol)	Grid box		Hydrogen Bond Interactions		Hydrophobic Interactions
				Center	Dimension	Amino Acid Residue	Distance (Å)	Amino Acid Residue
BCL2 (PDB ID:5VAU)	*Cinobufagin[23]	11,969,542	−8.4	X = -7.856 Y = 7.516 Z = 21.954	Size X = 40 Size Y = 40 Size Z = 40	Asn143, Lys117	3.19, 3.07	Asp121, Val118, Arg146, Lys117, Asp121, Ile125, Asn143, Arg146, Asp140
	*Nodakenetin[24]	26,305	−7.3	X = -7.856 Y = 7.516 Z = 21.954	Size X = 40 Size Y = 40 Size Z = 40	N/A	N/A	Glu165, Val162, Asn163, Trp176, Tyr180, Phe130, Ala131
	S55746	46,216,556	−14.0	X = -7.856 Y = 7.516 Z = 21.954	Size X = 40 Size Y = 40 Size Z = 40	Asn143	2.86	Val118, Lys117, Arg114, Asp140, Asp121
	A-1331852	71,565,985	−9.6	X = -7.856 Y = 7.516 Z = 21.954	Size X = 40 Size Y = 40 Size Z = 40	Arg146, Asp121	2.96, 3.04	Ile125, Asp121, Val118, Lys117, Val118, Arg114, Ile125, Asp124, Asp140
	WEHI-539 HCl	154,731,968	−9.4	X = -7.856 Y = 7.516 Z = 21.954	Size X = 40 Size Y = 40 Size Z = 40	Asn143, Asp124	3.16, 3.21	Val142, Trp88, Asn192, Gly128, Ile125, Asn111, Arg114, Asp121, Val118,
	BTSA1	3,857,348	−9.4	X = -7.856 Y = 7.516 Z = 21.954	Size X = 40 Size Y = 40 Size Z = 40	Arg146	3.00, 3.12	Asn143, Ile125, Lys117, Arg114, Val118, Asp121, Ile125, Val142, Asn143, Asp140, Arg146
	Unesbulin (PTC596)	74,223,469	−9.3	X = -7.856 Y = 7.516 Z = 21.954	Size X = 40 Size Y = 40 Size Z = 40	Asp121, Asp140	3.20, 3.08	Arg114, Lys117, Val118, Asn143, Asp121, Ile125, Lys117, Arg146
	VU661013	134,828,256	−9.0	X = -7.856 Y = 7.516 Z = 21.954	Size X = 40 Size Y = 40 Size Z = 40	N/A	N/A	Val118, Ile125, Arg114, Val142, Gly141, Asp140, Arg146, Asp140, Lys117, Asp121, Asn143
	Berberine chloride hydrate	155,074	−8.8	X = -7.856 Y = 7.516 Z = 21.954	Size X = 40 Size Y = 40 Size Z = 40	N/A	N/A	Arg127, Ala131, Trp176, Asn163, Val162, Ser167, Glu135, Tyr180, Glu165, Phe130
	Berberine chloride (NSC 646666)	12,456	−8.8	X = -7.856 Y = 7.516 Z = 21.954	Size X = 40 Size Y = 40 Size Z = 40	N/A	N/A	Trp176, Phe130, Arg127, Ala131, Asn163, Ser167, Glu135, Val162, Glu165, Tyr180
	Obatoclax Mesylate (GX15-070)	16,681,698	−8.6	X = -7.856 Y = 7.516 Z = 21.954	Size X = 40 Size Y = 40 Size Z = 40	Asp121	3.13	Lys117, Arg146, Asp140, Arg114, Lys117, Val118, Ile125, Asp121, Asn143
	Mifepristone (RU486)	55,245	−8.3	X = -7.856	Size X = 40	N/A	N/A	Glu135, Glu165, Tyr180,

(*continued on next page*)

Table 4 (*continued*)

Protein	Ligand	PubChem ID	Binding energy (kcal/mol)	Grid box		Hydrogen Bond Interactions		Hydrophobic Interactions
				Center	Dimension	Amino Acid Residue	Distance (Å)	Amino Acid Residue
				Y = 7.516 Z = 21.954	Size Y = 40 Size Z = 40			Asn163, Ala131, Thr132, Val162, Tyr28, Arg183
	BAM7	3,101,542	−8.3	X = -7.856 Y = 7.516 Z = 21.954	Size X = 40 Size Y = 40 Size Z = 40	Asn143, Asp140	3.27, 3.25	Ile25, Lys117, Arg114, Val118, Asp121, Val142, Ile125, Arg139, Arg146
	BDA-366	91,826,545	−7.5	X = -7.856 Y = 7.516 Z = 21.954	Size X = 40 Size Y = 40 Size Z = 40	Asp140, Asp121(E), Asp121(G) Arg146(C)	3.13, 3.29, 2.88, 3.05	Asp140, Arg146, Val118, Ile125, Arg114, Lys117, Arg114
	BAI1	2,729,026	−7.1	X = -7.856 Y = 7.516 Z = 21.954	Size X = 40 Size Y = 40 Size Z = 40	N/A	N/A	Arg114, Asp121, Val118, Asp121, Val118, Asn143
	HA14-1	3549	−6.4	X = -7.856 Y = 7.516 Z = 21.954	Size X = 40 Size Y = 40 Size Z = 40	Asp121, Arg146	3.00, 2.92	Asp140, Asn143, Ile125, Val118, Asp121, Lys117

*Cinobufagin: A natural inhibitor on BCL2; *Nodakenetin: A natural inhibitor on BCL2.

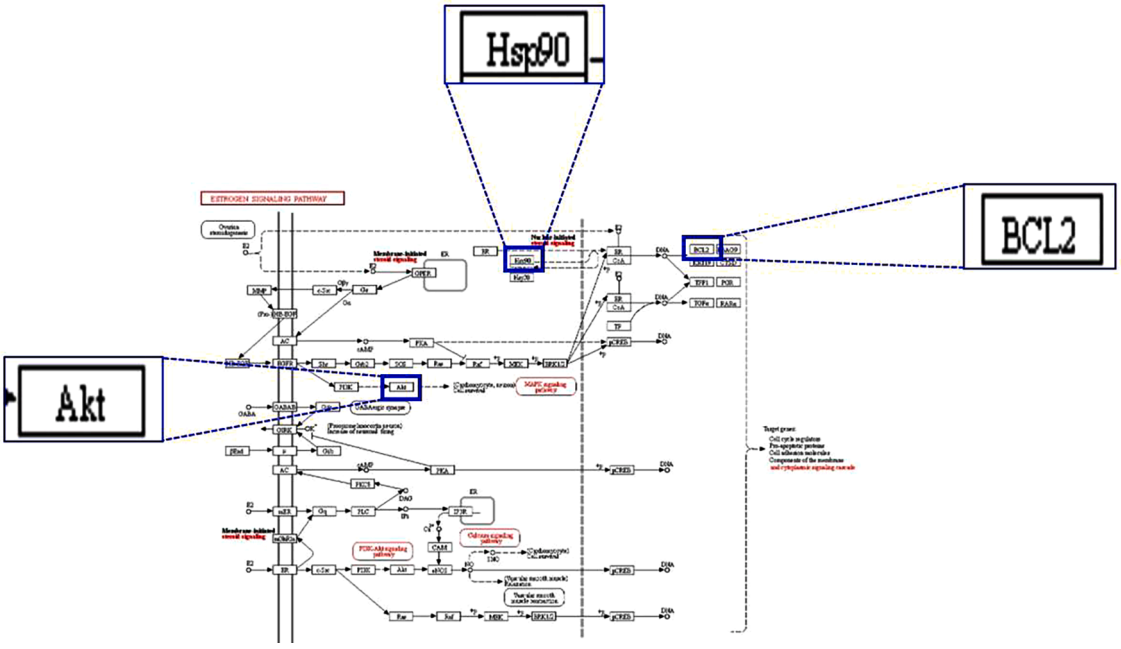

Fig. 4. Estrogen signaling pathway on KEGG enrichment diagram.

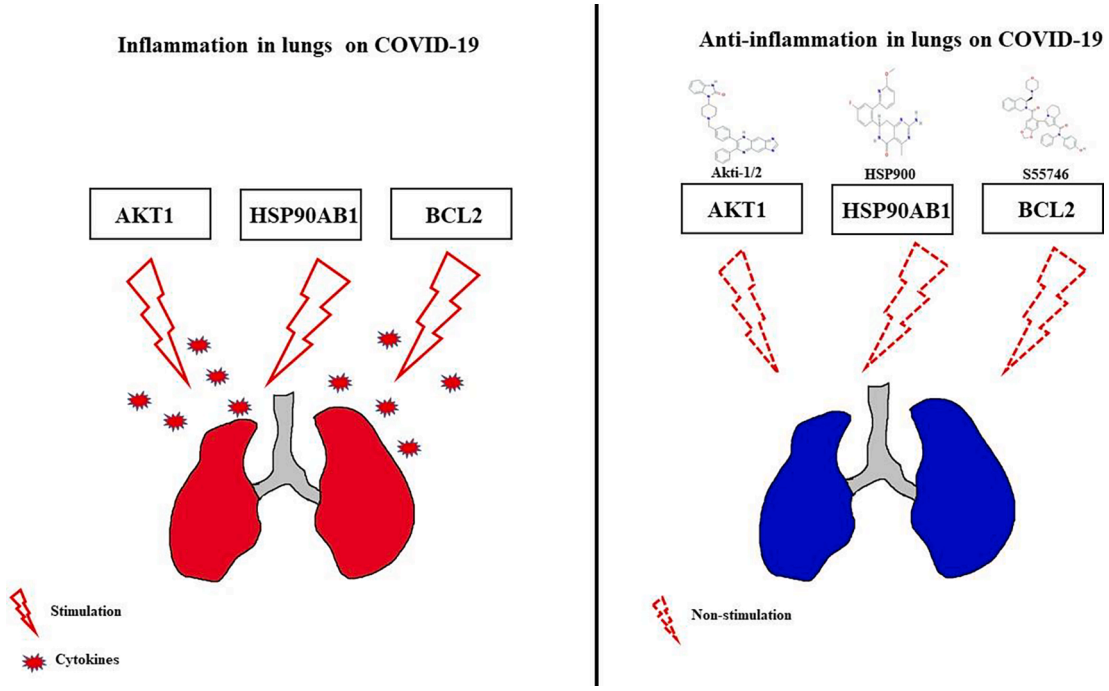

Fig. 5. Anti-inflammatory mechanism of promising three ligands in lungs on COVID-19.

the work reported in this paper.

Acknowledgements

This research was acknowledged by the Department of Bio-Health Convergence, College of Biomedical Science, Kangwon National University, Chuncheon 24341, Republic of Korea.

Appendix A. Supplementary data

Supplementary data to this article can be found online at https://doi.org/10.1016/j.mehy.2021.110656.

References

[1] Oh KK, Adnan M, Cho DH. Network pharmacology approach to decipher signaling pathways associated with target proteins of NSAIDs against COVID-19. Sci Rep 2021;11:9606. https://doi.org/10.1038/s41598-021-88313-5.
[2] Singh TU, Parida S, Lingaraju MC, Kesavan M, Kumar D, Singh RK. Drug repurposing approach to fight COVID-19. Pharmacol Rep 2020;72:1479–508. https://doi.org/10.1007/s43440-020-00155-6.
[3] Shereen MA, Khan S, Kazmi A, Bashir N, Siddique R. COVID-19 infection: Origin, transmission, and characteristics of human coronaviruses. J Adv Res 2020;24:91–8. https://doi.org/10.1016/j.jare.2020.03.005.
[4] Huang F, Zhang C, Liu Q, Zhao Y, Zhang Y, Qin Y, et al. Identification of amitriptyline HCl, flavin adenine dinucleotide, azacitidine and calcitriol as repurposing drugs for influenza A H5N1 virus-induced lung injury. PLoS Pathogens 2020;16. 10.1371/journal.ppat.1008341.
[5] Li G, De Clercq E. Therapeutic options for the 2019 novel coronavirus (2019-nCoV). Nat Rev Drug Disc 2020;19:149–50. https://doi.org/10.1038/d41573-020-00016-0.
[6] Battagello DS, Dragunas G, Klein MO, Ayub ALP, Velloso FJ, Correa RG. Unpuzzling COVID-19: Tissue-related signaling pathways associated with SARS-CoV-2 infection and transmission. Clin Sci 2020;134:2137–60. https://doi.org/10.1042/CS20200904.
[7] Wang Y, Li F, Zhang Y, Zhou Y, Tan Y, Chen Y, et al. Databases for the targeted COVID-19 therapeutics. Br J Pharmacol 2020;177:4999–5001. https://doi.org/10.1111/bph.15234.
[8] Bharti R, Shukla SK. Molecules against Covid-19: An in silico approach for drug development. J Electron Sci Technol 2021;19:100095. https://doi.org/10.1016/j.jnlest.2021.100095.
[9] D S, AL G, D L, A J, S W, J H-C, et al. STRING v11: protein-protein association networks with increased coverage, supporting functional discovery in genome-wide experimental datasets. Nucleic Acids Res 2019;47:D607–13. 10.1093/NAR/GKY1131.
[10] Khanal P, Patil BM, Chand J, Naaz Y. Anthraquinone derivatives as an immune booster and their therapeutic option against COVID-19. Nat Prod Bioprospect 2020;10:325–35. https://doi.org/10.1007/s13659-020-00260-2.
[11] Daina A, Michielin O, Zoete V. SwissADME: a free web tool to evaluate pharmacokinetics, drug-likeness and medicinal chemistry friendliness of small molecules. Sci Rep 2017 7:1 2017;7:1–13. 10.1038/srep42717.
[12] Matsson P, Kihlberg J. How big is too big for cell permeability? J Med Chem 2017;60:1662–4. https://doi.org/10.1021/acs.jmedchem.7b00237.
[13] Kovats S. Estrogen receptors regulate innate immune cells and signaling pathways. Cell Immunol 2015;294:63–9. https://doi.org/10.1016/j.cellimm.2015.01.018.
[14] Montopoli M, Zorzi M, Cocetta V, Prayer-Galetti T, Guzzinati S, Bovo E, et al. Clinical outcome of SARS-CoV-2 infection in breast and ovarian cancer patients who underwent antiestrogenic therapy. Ann Oncol 2021;32:676–7. https://doi.org/10.1016/j.annonc.2021.01.069.
[15] Rogel A, Willoughby JE, Buchan SL, Leonard HJ, Thirdborough SM, Al-Shamkhani A. Akt signaling is critical for memory CD8+ T-cell development and tumor immune surveillance. PNAS 2017;114:E1178–87. https://doi.org/10.1073/pnas.1611299114.
[16] Xia QD, Xun Y, Lu JL, Lu YC, Yang YY, Zhou P, et al. Network pharmacology and molecular docking analyses on Lianhua Qingwen capsule indicate Akt1 is a potential target to treat and prevent COVID-19. Cell Prolif, 2020;53. 10.1111/cpr.12949.
[17] Wyler E, Mösbauer K, Franke V, Diag A, Gottula LT, Arsiè R, et al. Transcriptomic profiling of SARS-CoV-2 infected human cell lines identifies HSP90 as target for COVID-19 therapy. IScience 2021;24:102151. https://doi.org/10.1016/j.isci.2021.102151.
[18] Hirano T, Murakami M. COVID-19: A new virus, but a familiar receptor and cytokine release syndrome. Immunity 2020;52:731–3. https://doi.org/10.1016/j.immuni.2020.04.003.
[19] Antonov A, Snead C, Gorshkov B, Antonova GN, Verin AD, Catravas JD. Heat shock protein 90 inhibitors protect and restore pulmonary endothelial barrier function. Am J Respir Cell Mol Biol 2008;39:551–9. https://doi.org/10.1165/rcmb.2007-0324OC.
[20] Hu C-A, Murphy I, Klimaj S, Reece J, Chand HS. SARS-CoV-2, inflammatory apoptosis, and cytokine storm syndrome. Open COVID J 2021;1:22–31. https://doi.org/10.2174/2666958702101010022.
[21] Costela-Ruiz VJ, Illescas-Montes R, Puerta-Puerta JM, Ruiz C, Melguizo-Rodríguez L. SARS-CoV-2 infection: The role of cytokines in COVID-19 disease. Cytokine Growth Factor Rev 2020;54:62–75. https://doi.org/10.1016/j.cytogfr.2020.06.001.
[22] Lim W, Yang C, Bazer FW, Song G. Luteolin inhibits proliferation and induces apoptosis of human placental choriocarcinoma cells by blocking the PI3K/AKT pathway and regulating sterol regulatory element binding protein activity. Biol Reprod 2016;95:82–3. 10.1095/BIOLREPROD.116.141556.
[23] Zhang G, Wang C, Sun M, Li J, Wang B, Jin C, et al. Cinobufagin inhibits tumor growth by inducing intrinsic apoptosis through AKT signaling pathway in human nonsmall cell lung cancer cells. Oncotarget 2016;7:28935–46.
[24] Dong L, Xu WW, Li H, Bi KH. In vitro and in vivo anticancer effects of marmesin in U937 human leukemia cells are mediated via mitochondrial-mediated apoptosis, cell cycle arrest, and inhibition of cancer cell migration. Oncol Rep 2018;39:597–602. https://doi.org/10.3892/OR.2017.6147.